

Additive Models for Symmetric Positive-Definite Matrices, Riemannian Manifolds and Lie groups

Zhenhua Lin^{1*}Hans-Georg Müller^{2†}Byeong U. Park^{3‡}¹*National University of Singapore*²*University of California, Davis*³*Seoul National University*

Abstract

In this paper an additive regression model for a symmetric positive-definite matrix valued response and multiple scalar predictors is proposed. The model exploits the abelian group structure inherited from either the Log-Cholesky metric or the Log-Euclidean framework that turns the space of symmetric positive-definite matrices into a Riemannian manifold and further a bi-invariant Lie group. The additive model for responses in the space of symmetric positive-definite matrices with either of these metrics is shown to connect to an additive model on a tangent space. This connection not only entails an efficient algorithm to estimate the component functions but also allows to generalize the proposed additive model to general Riemannian manifolds that might not have a Lie group structure. Optimal asymptotic convergence rates and normality of the estimated component functions are also established. Numerical studies show that the proposed model enjoys superior numerical performance, especially when there are multiple predictors. The practical merits of the proposed model are demonstrated by analyzing diffusion tensor brain imaging data.

Keywords: Riemannian manifold, Lie group, diffusion tensor, asymptotic normality, additive regression, Log-Euclidean metric, Log-Cholesky metric.

1 Introduction

Data in the form of symmetric positive-definite matrices arise in many areas, including computer vision (Caseiro et al., 2012; Rathi et al., 2007), signal processing (Arnaudon et al., 2013; Hua et al., 2017), medical imaging (Dryden et al., 2009; Fillard et al., 2007) and neuroscience (Friston, 2011), among other fields and

*Corresponding author; email: linz@nus.edu.sg. Research was partially supported by NUS startup grant R-155-000-217-133.

†Email: hgmueller@ucdavis.edu. Research was supported in part by NSF grant DMS-2014626.

‡Email: bupark@stats.snu.ac.kr. The work was supported by Samsung Science and Technology Foundation (project number SSTF-BA1802-01).

applications. For instance, they are used to model brain functional connectivity that is often characterized by covariance matrices of blood-oxygen-level dependent signals (Huettel et al., 2008). In diffusion tensor imaging analysis (Le Bihan, 1991), a 3×3 symmetric positive matrix that is computed for each voxel describes the dominant shape of local diffusion of water molecules.

The space \mathcal{S}^+ of symmetric positive matrices is a nonlinear metric space and, depending on the metric, forms a Riemannian manifold. Various metrics have been studied (Pigoli et al., 2014); one criterion for the choice of the metric is to avoid the swelling effect in the geodesics connecting two elements of \mathcal{S}^+ (Arsigny et al., 2007) that negatively affects the Frobenius metric and various other metrics. The abundance of \mathcal{S}^+ -valued data in many areas stands in contrast with the relative sparsity of work on their statistical analysis, in particular regarding regression with \mathcal{S}^+ -valued responses, which is the theme of this paper. Existing work includes Riemannian frameworks to analyze diffusion tensor images with a focus on averages and modes of variation (Fletcher and Joshi, 2007; Pennec et al., 2006) and various versions of nonparametric regression such as spline regression (Barmpoutis et al., 2007), local constant regression (Davis et al., 2010), intrinsic local linear regression (Yuan et al., 2012), wavelet regression (Chau and von Sachs, 2019) and Fréchet regression (Petersen et al., 2019). Various metric, manifold and Lie group structures have been proposed, for example, the trace metric (Lang, 1999), affine-invariant metric (also called Fisher–Rao metric) (Moakher, 2005; Pennec et al., 2006; Fletcher and Joshi, 2007), Log-Euclidean metric (Arsigny et al., 2007), Log-Cholesky metric (Lin, 2019), scaling-rotation distance (Jung et al., 2015) and Procrustes distance (Dryden et al., 2009). As the \mathcal{S}^+ manifold is a Riemannian manifold and more generally a metric space, regression techniques developed for general Riemannian manifolds (e.g., Pelletier, 2006; Shi et al., 2009; Steinke et al., 2010; Davis et al., 2010; Fletcher, 2013; Hinkle et al., 2014; Cornea et al., 2017, among many others) and metric spaces (Hein, 2009; Petersen and Müller, 2019; Lin and Müller, 2019) also apply to the \mathcal{S}^+ space.

Additive regression originated with Stone (1985) and is known to be an efficient way of avoiding the well known curse of dimensionality problem that one faces in nonparametric regression when the dimension of the covariate vector increases but so far has been by and large limited to the case of real-valued and functional responses. Examples for additive regression approaches for real-valued responses include the original work on smooth backfitting (Mammen et al., 1999), its extensions to generalized additive models (Yu et al., 2008), to additive quantile models (Lee et al., 2010), to generalized varying coefficient models (Lee et al., 2012), and to the case of errors-in-variables (Han and Park, 2018). Additive models for functional responses include additive functional regression based on spline basis representation (Scheipl et al., 2015), smooth backfitting via real-valued singular components (Park et al., 2018), and modeling density-valued responses (Han et al., 2020) with transformations (Petersen and Müller, 2016). Recently, a general framework for Hilbert-space-valued responses has been developed (Jeon and Park, 2020).

This paper contains three major contributions. First, to the best of our knowledge, this is the first paper to study additive regression for \mathcal{S}^+ -valued responses. As theoretically and numerically demonstrated below, additive regression is less prone to the curse of dimensionality while maintaining a high degree of

flexibility in the spirit of structured nonparametric modeling. In contrast, previous studies for modeling \mathcal{S}^+ -valued responses focused on “full” nonparametric regression such as local constant/polynomial regression that are well known to be subject to the curse of dimensionality when there are many predictors. Second, by focusing on the Log-Cholesky and Log-Euclidean frameworks that endow the space \mathcal{S}^+ with an abelian Lie group structure and a bi-invariant metric, we propose a novel intrinsic group additive regression model that exploits the abelian group structure of the manifold \mathcal{S}^+ in a regression setting for the first time. This sets our work apart, as previously only the general manifold structure of \mathcal{S}^+ was considered in regression approaches. Third, we show that this group additive model can be transformed into an additive model on tangent spaces by utilizing the Riemannian logarithmic map. This not only leads to an efficient way to estimate the additive component functions, but also paves the way for extending the additive model to other more general manifolds, leading to a general approach to manifold additive modeling.

2 Methodology

2.1 Preliminaries on Manifolds

The proposed approaches for manifold additive modeling are closely tied to the manifold structure of the response space in a general regression model, where we showcase the proposed approaches for the space \mathcal{S}^+ of symmetric positive-definite matrices. To properly define the proposed manifold additive models we require some basic notions for Riemannian manifolds and Lie groups that are compiled in the following. Let \mathcal{M} be a simply connected and smooth manifold modeled on a D -dimensional Euclidean space. The tangent space $T_y\mathcal{M}$ at $y \in \mathcal{M}$ is a linear space consisting of velocity vectors $\alpha'(0)$ where $\alpha : (-1, 1) \rightarrow \mathcal{M}$ represents a differentiable curve passing through y , i.e., $\alpha(0) = y$. Each tangent space $T_y\mathcal{M}$ is endowed with an inner product g_y that varies smoothly with y and thus is a D -dimensional Hilbert space with the induced norm denoted by $\|\cdot\|_y$. The inner products $\{g_y : y \in \mathcal{M}\}$ are collectively denoted by g , referred to as the Riemannian metric of \mathcal{M} that also defines a distance d on \mathcal{M} .

A geodesic γ is a curve defined on $[0, \infty)$ such that for each $t \in [0, \infty)$, $\gamma([t, t + \epsilon])$ is the shortest path connecting $\gamma(t)$ and $\gamma(t + \epsilon)$ for all sufficiently small $\epsilon > 0$. The Riemannian exponential map Exp_y at $y \in \mathcal{M}$ is a function mapping $T_y\mathcal{M}$ into \mathcal{M} and defined by $\text{Exp}_y(u) = \gamma(1)$ with $\gamma(0) = y$ and $\gamma'(0) = u \in T_y\mathcal{M}$. Conversely, $\gamma_{y,u}(t) = \text{Exp}_y(tu)$ is a geodesic starting at y and with direction u . For a tangent vector $u \in T_y\mathcal{M}$, the cut time c_u is the positive number such that $\gamma_{y,u}([0, c_u])$ is a shortest path connecting $\gamma_{y,u}(0)$ and $\gamma_{y,u}(c_u)$, but $\gamma_{y,u}([0, c_u + \epsilon])$ is not a shortest path for any $\epsilon > 0$. Let $\mathcal{E}_y = \{\text{Exp}_y(tu) : u \in T_y\mathcal{M}, \|u\|_y = 1, 0 \leq t < c_u\}$. The inverse of Exp_y , denoted by Log_y and called the Riemannian logarithmic map at y , can be defined by $\text{Log}_y z = u$ for $z \in \mathcal{E}_y$ such that $\text{Exp}_y u = z$.

A vector field U is a function defined on \mathcal{M} such that $U(y) \in T_y\mathcal{M}$. The Levi-Civita covariant derivative ∇ on \mathcal{M} is a torsion-free bilinear form that, at $y \in \mathcal{M}$, maps a tangent vector $v \in T_y\mathcal{M}$ and a vector field U to another tangent vector $\nabla_v U \in T_y\mathcal{M}$. Given a curve $\gamma(t)$ on \mathcal{M} , $t \in I$ for a real interval I , a vector field U

along γ is a smooth map defined on I such that $U(t) \in T_{\gamma(t)}\mathcal{M}$. We say U is parallel along γ if $\nabla_{\gamma'(t)}U = 0$ for all $t \in I$. In this paper, we primarily focus on parallel vector fields along geodesics. Let $\gamma : [0, 1] \rightarrow \mathcal{M}$ be a geodesic connecting y and z , and U a parallel vector field along γ such that $U(0) = u$ and $U(1) = v$. Then v is the parallel transport of u along γ , denoted by $\tau_{y,z}u = v$.

When \mathcal{M} is a group such that the group operation \oplus and inverse $\iota : y \mapsto y^{-1}$ are smooth, (\mathcal{M}, \oplus) is called a Lie group. The tangent space at the identity element e is a Lie algebra denoted by \mathfrak{g} . It consists of left-invariant vector fields U , i.e., $U(y \oplus z) = (DL_y)(U(z))$, where $L_y : z \mapsto y \oplus z$ and DL_y is the differential of L_y . A Riemannian metric g is called left-invariant if $g_z(u, v) = g_{y \oplus z}((DL_y)u, (DL_y)v)$ for all $y, z \in \mathcal{M}$ and $u, v \in T_z\mathcal{M}$, i.e., DL_y is an isometry for all $y \in \mathcal{M}$. Right-invariance can be defined in a similar fashion. A metric is bi-invariant if it is both left-invariant and right-invariant. The Lie exponential map, denoted by \mathbf{exp} that maps \mathfrak{g} into \mathcal{M} , is defined by $\mathbf{exp}(u) = \gamma(1)$ where $\gamma : \mathbb{R} \rightarrow \mathcal{M}$ is the unique one-parameter subgroup such that $\gamma'(0) = u \in \mathfrak{g}$. Its inverse, if it exists, is denoted by \mathbf{log} . When g is bi-invariant, then $\mathbf{exp} = \text{Exp}_e$, i.e., the Riemannian exponential map at the identity element coincides with the Lie exponential map.

2.2 Additive models for symmetric positive-definite matrices

The space of $m \times m$ symmetric positive-definite matrices \mathcal{S}_m^+ is a smooth submanifold of $\mathbb{R}^{m \times m}$, and its tangent spaces are identified with $\mathcal{S}(m)$, the collection of $m \times m$ symmetric matrices. Upon endowing the tangent spaces with a Riemannian metric g , \mathcal{S}_m^+ becomes a Riemannian manifold. We specifically focus on the Log-Cholesky (Lin, 2019) and Log-Euclidean (Arsigny et al., 2007) metrics while we also consider extensions to other metrics and general Riemannian manifolds. Each of these metrics is associated with a group operation \oplus that turns \mathcal{S}_m^+ into an abelian Lie group in which the metric is bi-invariant.

Example 1 (Log-Cholesky metric). Let $\text{LT}(m)$ be the space of $m \times m$ lower triangular matrices and $\text{LT}_+(m) \subset \text{LT}(m)$ the subspace such that $L \in \text{LT}_+(m)$ if all diagonal elements of L are positive. One can show that $\text{LT}_+(m)$ is a smooth submanifold of $\text{LT}(m)$ and its tangent spaces are identified with $\text{LT}(m)$. For a fixed $L \in \text{LT}_+(m)$, we define a Riemannian metric \tilde{g} on $\text{LT}_+(m)$ by $\tilde{g}_L(A, B) = \sum_{1 \leq j < i \leq m} A_{ij}B_{ij} + \sum_{j=1}^m A_{jj}B_{jj}L_{jj}^{-2}$, where A_{ij} denotes the element of A in the i th row and j th column. It is further turned into an abelian Lie group with the operation \odot defined by $L_1 \odot L_2 = \mathfrak{L}(L_1) + \mathfrak{L}(L_2) + \mathfrak{D}(L_1)\mathfrak{D}(L_2)$, where $\mathfrak{L}(L)$ is the strict lower triangular part of L , that is, $(\mathfrak{L}(L))_{ij} = L_{ij}$ if $j < i$ and $(\mathfrak{L}(L))_{ij} = 0$ otherwise, and $\mathfrak{D}(L)$ is the diagonal part of L , that is, a diagonal matrix whose diagonals are equal to the respective diagonals of L . One can show that \tilde{g} is a bi-invariant metric for the Lie group $\text{LT}_+(m)$ with the group operation \odot . It is well known that a symmetric positive-definite matrix P is associated with a unique matrix L in $\text{LT}_+(m)$ such that $LL^\top = P$. This L is called the Cholesky factor of P in this paper. For $U, V \in T_P\mathcal{S}_m^+ = \mathcal{S}(m)$, we define the metric $g_P(U, V) = \tilde{g}_L(L(L^{-1}UL^{-\top})_{\frac{1}{2}}, L(L^{-1}VL^{-\top})_{\frac{1}{2}})$, where $(S)_{\frac{1}{2}} = \mathfrak{L}(S) + \mathfrak{D}(S)/2$ for a matrix S . We also turn \mathcal{S}_m^+ into an abelian Lie group with the operator \oplus such that $P_1 \oplus P_2 = (L_1 \odot L_2)(L_1 \odot L_2)^\top$, where L_1 and L_2 are the Cholesky factors of P_1 and P_2 , respectively. The metric g is a bi-invariant metric of the Lie group \mathcal{S}_m^+ with the group operation \oplus .

Example 2 (Log-Euclidean metric). For a symmetric matrix S , $\exp(S) = I_m + \sum_{j=1}^{\infty} \frac{1}{j!} S^j$ is a symmetric positive-definite matrix. For a symmetric positive-definite matrix P , the matrix logarithmic map is $\log(P) = S$ such that $\exp(S) = P$. The log map is a smooth map from the manifold \mathcal{S}_m^+ to the space $\mathcal{S}(m)$. The operation \oplus defined as $P_1 \oplus P_2 = \exp(\log(P_1) + \log(P_2))$ turns \mathcal{S}_m^+ into an abelian group. Define $g_P(U, V) = \text{trace} \left[((D_P \log)U)((D_P \log)V) \right]$, where $D_P \log$ denotes the differential of the log map at P . This is a bi-invariant metric on \mathcal{S}_m^+ with the group operation \oplus .

For random elements $Y \in \mathcal{S}_m^+$ we define the Fréchet function $F(y) = \mathbb{E}d^2(y, Y)$, where d is the Riemannian distance function induced by the Log-Cholesky or the Log-Euclidean metric. If $F(y) < \infty$ for some $y \in \mathcal{S}_m^+$ and hence $F(y) < \infty$ for all $y \in \mathcal{S}_m^+$ according to the triangle inequality, we say Y is of the second order. If Y is a second-order element in \mathcal{S}_m^+ , then the minimizer of $F(y)$, called the Fréchet mean, exists and is unique. This follows from the fact that both Log-Cholesky and Log-Euclidean metrics turn \mathcal{S}_m^+ into a Hadamard manifold, i.e., a simply connected Riemannian manifold that is also a Hadamard space; Sturm (2003) showed that the Fréchet mean exists and is unique for such spaces.

Given scalar variables $X_1 \in \mathcal{X}_1, \dots, X_q \in \mathcal{X}_q$, which are predictors that are paired with a manifold-valued response Y and where $\mathcal{X}_j \subset \mathbb{R}$, $j = 1, \dots, q$, are their domains, we are now in a position to formulate the proposed manifold additive model as follows,

$$Y = \mu \oplus w_1(X_1) \oplus \dots \oplus w_q(X_q) \oplus \zeta, \quad (1)$$

where μ is the Fréchet mean of Y , each w_k is a function that maps X_k into \mathcal{M} , ζ is random noise which has a Fréchet mean that corresponds to the group identity element e , and \mathcal{X}_k are compact domains of \mathbb{R} . The above model generalizes the additive model for vector-valued response to \mathcal{S}_m^+ -valued and more generally Lie group responses. It includes noise impacting the responses, which cannot be additively modeled in the absence of a linear structure; the effect of the mean response and of the additive component functions, which again cannot be additively modeled. The Lie group operation is the natural way to substitute for the addition operation in Euclidean spaces when responses lie in a Lie group.

The statistical task is now to estimate the unknown parameter μ and the component functions w_1, \dots, w_q , given a sample of independently and identically distributed (i.i.d.) observations of size n . This is challenging due to the lack of a linear structure in \mathcal{S}_m^+ or more generally, for any general Lie group elements. The following crucial observation about the model is the key to tackle this challenge.

Proposition 1. *If (\mathcal{M}, \oplus) is an abelian Lie group endowed with a bi-invariant metric g that turns \mathcal{M} into a Hadamard manifold, then (1) is equivalent to*

$$\text{Log}_\mu Y = \sum_{k=1}^q \tau_{e,\mu} \mathbf{log} w_k(X_k) + \tau_{e,\mu} \mathbf{log} \zeta. \quad (2)$$

Let $f_k(X_k) = \tau_{e,\mu} \mathbf{log} w_k(X_k)$ and $\varepsilon = \tau_{e,\mu} \mathbf{log} \zeta$. Then according to Proposition 1, one may rewrite the

model (1) as

$$\text{Log}_\mu Y = \sum_{k=1}^q f_k(X_k) + \varepsilon \quad (3)$$

with $\mathbb{E}\varepsilon = \mathbb{E}\tau_{e,\mu} \log \zeta = \tau_{e,\mu} \mathbb{E} \log \zeta = 0$. We also note that $\mathbb{E}(\sum_{k=1}^q f_k(X_k)) = 0$ since $\mathbb{E} \text{Log}_\mu Y = 0$. For the identifiability of the individual component functions f_k , we assume that $\mathbb{E} f_k(X_k) = 0$. This is equivalent to assuming that the Fréchet mean of each $w_k(X_k)$ in (1) equals the group identity element e . These considerations motivate to estimate the component functions w_k through estimation of the f_k , as follows.

Step 1: Compute the sample Fréchet mean $\hat{\mu}$. Closed-form expressions of $\hat{\mu}$ are available for many special cases including the Log-Cholesky and Log-Euclidean metrics.

Step 2: Compute $\text{Log}_{\hat{\mu}} Y_i$. There is also a closed-form expression available for the Log-Cholesky metric. For the Log-Euclidean metric, there is no closed-form expression, and a numerical approach is required.

Step 3: Solve the system of integral equations

$$\hat{f}_k(x_k) = \hat{m}_k(x_k) - n^{-1} \sum_{i=1}^n \text{Log}_{\hat{\mu}} Y_i - \sum_{j:j \neq k} \int_{\mathcal{X}_j} \hat{f}_j(x_j) \frac{\hat{p}_{kj}(x_k, x_j)}{\hat{p}_k(x_k)} dx_j, \quad 1 \leq k \leq q, \quad (4)$$

subject to the constraints $\int_{\mathcal{X}_j} \hat{f}_k(x_k) \hat{p}_k(x_k) dx_k = 0$ for $1 \leq k \leq q$. Here, $\hat{p}_k(x_k) = n^{-1} \sum_{i=1}^n K_{h_k}(x_k, X_{ik})$, $\hat{p}_{kj}(x_k, x_j) = n^{-1} \sum_{i=1}^n K_{h_k}(x_k, X_{ik}) K_{h_j}(x_j, X_{ij})$, and

$$\hat{m}_k(x_k) = n^{-1} \hat{p}_k(x_k)^{-1} \sum_{i=1}^n K_{h_k}(x_k, X_{ik}) \text{Log}_{\hat{\mu}} Y_i. \quad (5)$$

Here K_{h_j} is a kernel function with $\int_{\mathcal{X}_j} K_{h_j}(u, v) du = 1$ for all $v \in \mathcal{X}_j$, see [Jeon and Park \(2020\)](#). Note that $n^{-1} \sum_{i=1}^n \text{Log}_{\hat{\mu}} Y_i = 0$ since $\hat{\mu}$ is the sample Fréchet mean.

Step 4: Finally, estimate $w_k(x_k)$ by $\hat{w}_k(x_k) = \exp\{\tau_{\hat{\mu}, e} \hat{f}_k(x_k)\}$.

Step 3 is a multivariate version of the standard Smooth Backfitting (SBF) system of equations ([Mammen et al., 1999](#)). Since the tangent space $T_{\hat{\mu}} \mathcal{S}_m^+$ is also a Hilbert space, the above SBF system of equations can be interpreted from a Bochner integral perspective, see [Jeon and Park \(2020\)](#), where also the empirical selection of bandwidths h_k is discussed.

2.3 Extension to general manifolds

When \mathcal{S}_m^+ is endowed with another metric, such as the affine-invariant metric ([Moakher, 2005](#); [Pennec et al., 2006](#); [Fletcher and Joshi, 2007](#)), it is no longer an abelian group with a bi-invariant metric, and Proposition 1 does not hold. However, model (3) might still apply, since it depends only on two ingredients, the existence and uniqueness of the Fréchet mean μ , and the well-definedness of $\text{Log}_\mu Y$. These ingredients are satisfied

for \mathcal{S}_m^+ endowed with the affine-invariant metric, for which \mathcal{S}_m^+ becomes a Hadamard manifold. For general metrics that might feature positive sectional curvature, or more generally, for manifolds beyond \mathcal{S}_m^+ , we require additional conditions for model (3) to be applicable, as follows.

Let (\mathcal{M}, g) now denote a general Riemannian manifold and Y a random element on \mathcal{M} . Assume that:

(A1) The minimizer of F exists and is unique.

As previously mentioned, this condition is satisfied when \mathcal{M} is a Hadamard manifold. For other manifolds, we refer readers to [Bhattacharya and Patrangenaru \(2003\)](#) and [Afsari \(2011\)](#) for conditions that imply (A1).

For a nonempty subset $A \subset \mathcal{M}$, let $d(y, A) = \inf\{d(y, z) : z \in A\}$ be the distance between y and the set A . For a positive real number ϵ , we denote $A^\epsilon = \{y : d(y, A) < \epsilon\}$ and $A^{-\epsilon} = \mathcal{M} \setminus (\mathcal{M} \setminus A)^\epsilon$. When $A = \emptyset$, set $A^\epsilon = \emptyset$. We make the following assumption; it is not needed for the case of a Hadamard manifold.

(A2) $\Pr\{Y \in \mathcal{E}_\mu^{-\epsilon_0}\} = 1$ for some $\epsilon_0 > 0$, where \mathcal{E}_μ is defined in [Section 2.1](#).

If (A1) and (A2) are satisfied, the proposed manifold additive model (3) remains well defined, and the first three steps of the estimation method described in the previous subsection are still valid and can be employed to estimate f_1, \dots, f_q , with \mathcal{S}_m^+ replaced by \mathcal{M} .

3 Theory

We first establish convergence rates and asymptotic normality of the estimators for the mean and the component functions for general manifolds in the manifold additive model (3) and then provide additional details for the space \mathcal{S}_m^+ endowed with either the Log-Cholesky metric or the Log-Euclidean metric. We consider a manifold \mathcal{M} that satisfies at least one of the following two properties but not necessarily both.

(M1) \mathcal{M} is a finite-dimensional Hadamard manifold that has sectional curvature bounded from below by $\mathfrak{c}_0 \leq 0$.

(M2) \mathcal{M} is a complete compact Riemannian manifold.

The space \mathcal{S}_m^+ with the Log-Cholesky metric, Log-Euclidean metric or affine-invariant metric is a manifold that satisfies (M1), while the unit sphere that is used to model compositional data ([Dai and Müller, 2018](#)) serves as an example of a manifold that satisfies (M2).

To establish the convergence rate of $\hat{\mu}$, we also make the following assumptions.

(A3) The manifold \mathcal{M} satisfies at least one of the conditions (M1) and (M2).

(A4) For some constant $\mathfrak{c}_2 > 0$, $F(y) - F(\mu) \geq \mathfrak{c}_2 d^2(y, \mu)$ when $d(y, \mu)$ is sufficiently small.

(A5) For some constant $\mathfrak{c}_3 > 0$, for all $y, z \in \mathcal{M}$, the linear operator $H_{y,z} : T_z\mathcal{M} \rightarrow T_z\mathcal{M}$, defined by $g_z(H_{y,z}u, v) = g_z(\nabla_u \text{Log}_z y, v)$ for $u, v \in T_z\mathcal{M}$, has its operator norm bounded by $\mathfrak{c}_3\{1 + d(z, y)\}$.

The operator $H_{y,z}$ in the technical condition (A5) is indeed the Hessian of the squared distance function d ; see also the equation (5.4) of Kendall and Le (2011). It is superfluous if the manifold \mathcal{M} is compact, and is satisfied by manifolds of zero curvature. It can also be replaced by a uniform moment condition on the operator norm of $H_{z,Y}$ over all z in a small local neighborhood of μ . We then obtain a parametric convergence rate for the Fréchet mean estimates $\hat{\mu}$.

Proposition 2. *Assume that (A1), (A3) and (A4) hold and Y is of the second order. Then $d(\hat{\mu}, \mu) = O_P(n^{-1/2})$.*

To obtain convergence rates of the estimated component functions, we require some additional conditions that are standard in the literature on additive regression.

- (B1) The kernel function K is positive, symmetric, Lipschitz continuous and supported on $[-1, 1]$.
- (B2) The bandwidths h_k satisfy $n^{1/5}h_k \rightarrow \alpha_k > 0$.
- (B3) The joint density p of X_1, \dots, X_q is bounded away from zero and infinity on $\mathcal{X} \equiv \mathcal{X}_1 \times \dots \times \mathcal{X}_q$. The densities p_{kj} are continuously differentiable for $1 \leq j \neq k \leq q$.
- (B4) The additive functions f_k are twice continuously (Fréchet) differentiable.

Without loss of generality, assume $\mathcal{X}_k = [0, 1]$ for all k and let $\mathcal{I}_k = [2h_k, 1 - 2h_k]$. The moment condition on ε in the following theorem is required to control the effect of the error of $\hat{\mu}$ as an estimator of μ on the discrepancies of $\text{Log}_{\hat{\mu}} Y_i$ from $\text{Log}_{\mu} Y_i$ after parallel transportation, see Lemma 2. It is a mild requirement and is satisfied for example when the manifold is compact or $\|\varepsilon\|_{\mu}$ follows a sub-exponential distribution.

Theorem 1. *Assume that the conditions (A1)–(A5) and (B1)–(B4) are satisfied, that $\mathbb{E}\|\varepsilon\|_{\mu}^{\alpha} < \infty$ for some $\alpha \geq 10$ and that $\mathbb{E}(\|\varepsilon\|_{\mu}^2 | X_j = \cdot)$ are bounded on \mathcal{X}_j , respectively, for $1 \leq j \leq q$. Then,*

$$\begin{aligned} \max_{1 \leq k \leq q} \int_{\mathcal{I}_k} \|\tau_{\hat{\mu}, \mu} \hat{f}_k(x_k) - f_k(x_k)\|_{\mu}^2 p_k(x_k) dx_k &= O_P(n^{-4/5}), \\ \max_{1 \leq k \leq q} \int_{\mathcal{X}_k} \|\tau_{\hat{\mu}, \mu} \hat{f}_k(x_k) - f_k(x_k)\|_{\mu}^2 p_k(x_k) dx_k &= O_P(n^{-3/5}), \end{aligned}$$

where $\tau_{\hat{\mu}, \mu}$ is the parallel transport operator along geodesics.

The following corollary is an immediate consequence.

Corollary 1. *Under the conditions of Theorem 1, if the \mathcal{M} is \mathcal{S}_m^+ endowed with either the Log-Cholesky metric or the Log-Euclidean metric, then*

$$\begin{aligned} \max_{1 \leq k \leq q} \int_{\mathcal{I}_k} \|\log \hat{w}_k(x_k) - \log w_k(x_k)\|_e^2 p_k(x_k) dx_k &= O_P(n^{-4/5}), \\ \max_{1 \leq k \leq q} \int_{\mathcal{X}_k} \|\log \hat{w}_k(x_k) - \log w_k(x_k)\|_e^2 p_k(x_k) dx_k &= O_P(n^{-3/5}). \end{aligned}$$

To derive the asymptotic distribution of \hat{f}_k , we define $\mathcal{C}_k(x) = \mathbb{E}\{\varepsilon \otimes \varepsilon \mid X_k = x\}$, where $u \otimes v : T_\mu \mathcal{M} \rightarrow T_\mu \mathcal{M}$ is a tensor product operator such that $(u \otimes v)z = g_\mu(u, z)v$. In addition, define

$$\Sigma_k(x) = \alpha_k^{-1} p_k(x)^{-1} \int K(u)^2 du \cdot \mathcal{C}_k(x), \quad (6)$$

$$\delta_k(x) = \frac{p'_k(x)}{p_k(x)} \int u^2 K(u) du \cdot f'_k(x), \quad (7)$$

$$\delta_{jk}(u, v) = \frac{\partial p_{jk}(u, v)}{\partial v} \frac{1}{p_{jk}(u, v)} \int u^2 K(u) du \cdot f'_k(v), \quad (8)$$

$$\tilde{\Delta}_k(x) = \alpha_k^2 \cdot \delta_k(x) + \sum_{j:j \neq k} \alpha_j^2 \int_{\mathcal{X}_j} \frac{p_{kj}(x, u)}{p_k(x)} \cdot \delta_{kj}(x, u) du, \quad (9)$$

where α_k are the constants in the condition (B2). Let $(\Delta_1, \dots, \Delta_q)$ be a solution of the system of equations

$$\Delta_k(x) = \tilde{\Delta}_k(x) - \sum_{j:j \neq k} \int_{\mathcal{X}_j} \frac{p_{kj}(x, u)}{p_k(x)} \cdot \Delta_j(u) du, \quad 1 \leq k \leq q, \quad (10)$$

satisfying the constraints

$$\int_{\mathcal{X}_k} p_k(x) \cdot \Delta_k(x) dx = \alpha_k^2 \cdot \int_{\mathcal{X}_k} p_k(x) \cdot \delta_k(x) dx, \quad 1 \leq k \leq q. \quad (11)$$

Finally, define $c_k(x) = \frac{1}{2} \int u^2 K(u) du \cdot f''_k(x)$ and $\theta_k(x) = \alpha_k^2 \cdot c_k(x) + \Delta_k(x)$.

We assume that

(B5) $\mathbb{E}\{\varepsilon \otimes \varepsilon \mid X_k = \cdot\}$ are continuous operators on \mathcal{X}_k for all $1 \leq k \leq q$ and operators $\mathbb{E}\{\varepsilon \otimes \varepsilon \mid X_j = \cdot, X_k = \cdot\}$ are bounded on $\mathcal{X}_j \times \mathcal{X}_k$ for all $1 \leq j \neq k \leq q$.

(B6) $\partial p / \partial x_k$, $k = 1, \dots, q$, exist and are bounded on $\mathcal{X} = \prod_{k=1}^q \mathcal{X}_k$.

Note that condition (B5) is superfluous if the random noise ε is independent of the predictors X_1, \dots, X_q .

Let $N_\mu(\mathbf{x})$ be the product measure $N(\theta_1(x_1), \Sigma_1(x_1)) \times \dots \times N(\theta_q(x_q), \Sigma_q(x_q))$ on $(T_\mu \mathcal{M})^q$, where $N(\theta, \Sigma)$ denotes a Gaussian measure on $T_\mu \mathcal{M}$ with the mean vector θ and covariance operator Σ . For a set A , let $\text{Int}(A)$ denote the interior of A .

Theorem 2. *Assume that conditions (A1)–(A5) and (B1)–(B6) hold, that $\mathbb{E}\|\varepsilon\|_\mu^\alpha < \infty$ for some $\alpha > 10$ and that there exists $\alpha' > 5/2$ such that $\mathbb{E}(\|\varepsilon\|_\mu^{\alpha'} \mid X_k = \cdot)$ are bounded on \mathcal{X}_k for all $1 \leq k \leq q$. Then, for $\mathbf{x} = (x_1, \dots, x_q) \in \text{Int}(\mathcal{X})$, it holds that $(n^{2/5}(\tau_{\hat{\mu}, \mu} \hat{f}_k(x_k) - f_k(x_k)) : 1 \leq k \leq q) \rightarrow N_\mu(\mathbf{x})$ in distribution. In addition, $n^{2/5} \left(\sum_{k=1}^q \tau_{\hat{\mu}, \mu} \hat{f}_k(x_k) - \sum_{k=1}^q f_k(x_k) \right)$ converges to $N_\mu(\theta(\mathbf{x}), \Sigma(\mathbf{x}))$, where $\theta(\mathbf{x}) = \sum_{k=1}^q \theta_k(x_k)$ and $\Sigma(\mathbf{x}) = \Sigma_1(x_1) + \dots + \Sigma_q(x_q)$.*

When \mathcal{M} is \mathcal{S}_m^+ equipped with either the Log-Cholesky metric or the Log-Euclidean metric, the above asymptotic normality can be formulated on the Lie algebra \mathfrak{g} . To this end, assume that $\Sigma_1^{\text{SPD}}, \dots, \Sigma_q^{\text{SPD}}$ and $\Delta_1^{\text{SPD}}, \dots, \Delta_q^{\text{SPD}}$ are defined by equations (6)–(11) with $\mathcal{C}_k(x)$ and f_k replaced by $\mathbb{E}\{\log \zeta \otimes \log \zeta \mid X_k = x\}$ and

$\psi_k := \mathbf{log} w_k$, respectively. Also, let $c_k^{\text{SPD}} = \frac{1}{2} \int u^2 K(u) du \cdot \psi_k''(x)$ and $\theta_k^{\text{SPD}}(x) = \alpha_k^2 \cdot c_k^{\text{SPD}}(x) + \Delta_k^{\text{SPD}}(x)$, for $k = 1, \dots, q$. The following corollary is an immediate consequence of Theorem 2, by noting that the manifold \mathcal{S}_m^+ when equipped with the Log-Cholesky metric or the Log-Euclidean metric satisfies the conditions (A1)–(A4) when the second moment of the random noise ζ is finite.

Corollary 2. *Assume that the conditions (B1)–(B6) hold and that $\mathbb{E}\|\mathbf{log}\zeta\|_\mu^\alpha < \infty$ for some $\alpha > 10$. Furthermore, assume that there exists $\alpha' > 5/2$ such that $\mathbb{E}(\|\mathbf{log}\zeta\|_e^{\alpha'} \mid X_k = \cdot)$ are bounded on \mathcal{X}_k for all $1 \leq k \leq q$. For \mathcal{S}_m^+ endowed with either the Log-Cholesky metric or the Log-Euclidean metric, for $\mathbf{x} = (x_1, \dots, x_q) \in \text{Int}(\mathcal{X})$, it holds that $(n^{2/5}(\mathbf{log}\hat{w}_k(x_k) - \mathbf{log}w_k(x_k)) : 1 \leq k \leq q) \rightarrow N_{I_m}(\mathbf{x})$ in distribution. In addition, $n^{2/5}(\sum_{k=1}^q \mathbf{log}\hat{w}_k(x_k) - \sum_{k=1}^q \mathbf{log}w_k(x_k))$ converges to $N_{I_m}(\theta(\mathbf{x}), \Sigma(\mathbf{x}))$, where I_m is the $m \times m$ identity matrix, $\theta(\mathbf{x}) = \sum_{k=1}^q \theta_k^{\text{SPD}}(x_k)$ and $\Sigma(\mathbf{x}) = \Sigma_1^{\text{SPD}}(x_1) + \dots + \Sigma_q^{\text{SPD}}(x_q)$.*

4 Simulations

To illustrate the numerical performance of the proposed manifold additive model estimators, we conducted simulations for $\mathcal{M} = \mathcal{S}_m^+$ for $m = 3$ endowed with the Log-Cholesky metric. We set $\mathcal{X}_k = [0, 1]$ for $k = 1, \dots, q$. The predictors X_1, \dots, X_k are independently and identically sampled from the uniform distribution on $[0, 1]$. We also fix μ to be the identity matrix. We then generate the response variable Y by $Y = \mu \oplus w(X_1, \dots, X_q) \oplus \zeta$, where $w(X_1, \dots, X_q) = \mathbf{exp}\tau_{\mu, e}f(X_1, \dots, X_q)$ with three settings for f :

- I. $f(x_1, \dots, x_q) = \sum_{k=1}^q f_k(x_k)$ with $f_k(x_k)$ being an $m \times m$ matrix whose (j, l) -entry is $g(x_k; j, l, q) = \exp(-|j - l|/q) \sin(2q\pi(x_k - (j + l)/q))$;
- II. $f(x_1, \dots, x_q) = f_{12}(x_1, x_2) + \sum_{k=3}^q f_k$, where f_k is defined as in the setting I, while $f_{12}(x_1, x_2)$ is an $m \times m$ matrix whose (j, l) -entry is $g(x_1; j, l, q)g(x_2, j, l, q)$;
- III. $f(x_1, \dots, x_q) = f_{12}(x_1, x_2) \prod_{k=3}^q f_k(x_k)$, where $f_{12}(x_1, x_2)$ is an $m \times m$ matrix whose (j, l) -entry is $\exp\{-(j + l)(x_1 + x_2)\}$, and $f_k(x_k)$ is an $m \times m$ matrix whose (j, l) -entry is $\sin(2\pi x_k)$.

The random noise ζ is generated according to $\mathbf{log}\zeta = \sum_{j=1}^6 Z_j v_j$, where Z_1, \dots, Z_6 are independently sampled from $N(0, \sigma^2)$, and v_1, \dots, v_6 are an orthonormal basis of the tangent space $T_e \mathcal{S}_m^+$. The signal-to-ratio (SNR) is measured by $\text{SNR} = \mathbb{E}\|\mathbf{log}w(X_1, \dots, X_q)\|_e^2 / \mathbb{E}\|\mathbf{log}\zeta\|_e^2$. We tweak the value of the parameter σ^2 to cover two settings for the SNR, namely, $\text{SNR} = 2$ and $\text{SNR} = 4$. We note that the model for f in I is an additive model, while models II and III are not additive. In particular, model III has no additive components and thus represents the most challenging scenario for the proposed additive regression. We consider $q = 3$ and $q = 4$ to probe the effect of the dimensionality of the predictor vector and sample sizes $n = 50, 100, 200$.

The quality of the estimation is measured by the prediction root mean squared error on an independent

Table 1: Prediction RMSE and its Monte Carlo standard error

Setting	q	n	MAM		ILPR	
			SNR=2	SNR=4	SNR=2	SNR=4
I	3	50	0.591 (0.056)	0.508 (0.057)	1.046 (0.147)	1.042 (0.146)
		100	0.413 (0.026)	0.339 (0.020)	0.912 (0.076)	0.909 (0.092)
		200	0.300 (0.017)	0.230 (0.012)	0.787 (0.030)	0.785 (0.050)
	4	50	0.772 (0.062)	0.685 (0.063)	1.075 (0.100)	1.056 (0.100)
		100	0.523 (0.029)	0.436 (0.036)	0.964 (0.033)	0.952 (0.040)
		200	0.354 (0.019)	0.284 (0.013)	0.918 (0.026)	0.902 (0.024)
II	3	50	0.624 (0.029)	0.581 (0.024)	0.948 (0.208)	0.914 (0.208)
		100	0.544 (0.017)	0.516 (0.013)	0.769 (0.078)	0.755 (0.195)
		200	0.498 (0.009)	0.481 (0.008)	0.645 (0.048)	0.624 (0.115)
	4	50	0.687 (0.035)	0.619 (0.032)	1.069 (0.150)	1.054 (0.158)
		100	0.553 (0.023)	0.503 (0.018)	0.933 (0.088)	0.924 (0.095)
		200	0.471 (0.014)	0.438 (0.010)	0.862 (0.045)	0.838 (0.040)
III	3	50	0.801 (0.067)	0.789 (0.065)	0.808 (0.220)	0.791 (0.269)
		100	0.750 (0.045)	0.744 (0.045)	0.681 (0.210)	0.688 (0.258)
		200	0.725 (0.050)	0.721 (0.050)	0.489 (0.083)	0.467 (0.138)
	4	50	0.871 (0.079)	0.866 (0.079)	1.000 (0.237)	1.009 (0.272)
		100	0.871 (0.077)	0.870 (0.078)	0.874 (0.191)	0.891 (0.230)
		200	0.857 (0.063)	0.857 (0.064)	0.776 (0.115)	0.776 (0.139)

test dataset of 1000 observations, defined by

$$\text{RMSE} = \sqrt{\frac{1}{1000} \sum_{i=1}^{1000} d^2(\hat{\mu} \oplus \hat{w}_1(\tilde{x}_{i1}) \oplus \cdots \oplus \hat{w}_q(\tilde{x}_{iq}), \tilde{Y}_i)},$$

where $(\tilde{x}_{i1}, \dots, \tilde{x}_{iq}, \tilde{Y}_i)$, $i = 1, \dots, 1000$, are i.i.d. observations in the test data. As a comparison method for the proposed manifold additive model (MAM), we also implement the intrinsic local polynomial regression (ILPR) proposed in Yuan et al. (2012), which is a fully nonparametric approach. Each simulation setting is repeated 100 times, and the Monte Carlo prediction RMSE and its standard error are shown in Table 1.

These results lead to the following observations. First, as $q = 3$ is increased to $q = 4$, the prediction RMSE of both methods increases for most cases, with the increase of ILPR much more prominent in almost all cases. This suggests that MAM is less subject to the curse of dimensionality. Second, when the model is correctly specified as in Setting I, the proposed model outperforms ILPR by a significant margin. When the underlying model is not a fully additive model but contains some additive components, such as the model in Setting II, the MAM approach still clearly outperforms ILPR. When the true model has no additive components, the fully nonparametric approach ILPR is favored in some cases, especially when $q = 3$. However, in the case $q = 4$ and the sample size is relatively small, i.e., $n = 50$ or $n = 100$, the additive model still enjoys

better performance even if misspecified. In summary, when there are several predictors or the sample size is relatively small, the additive model is often preferable, and when the number of predictors is limited or the sample size is large, a fully nonparametric approach can be competitive.

5 Application to Diffusion Tensor Imaging

We apply the proposed additive model to study diffusion tensors from Alzheimer’s Disease Neuroimaging Initiative¹ (ADNI). Diffusion tensors are 3×3 symmetric positive-definite matrices that characterize diffusion of water molecules in tissues and convey rich information about brain tissues with important applications in tractography. They are utilized to investigate the integrity of axons and to aid in the diagnosis of brain related diseases. In statistical modeling, diffusion tensors are typically considered to be random elements in the space $\mathcal{S}_3^+ \subset \mathcal{S}$, and were studied by [Fillard et al. \(2005\)](#); [Arsigny et al. \(2006\)](#); [Lenglet et al. \(2006\)](#); [Penneec \(2006\)](#); [Zhou et al. \(2016\)](#); [Fletcher and Joshi \(2007\)](#); [Dryden et al. \(2009\)](#); [Zhu et al. \(2009\)](#); [Penneec \(2020\)](#), among many others. A traditional Euclidean framework for diffusion tensors suffers from significant swelling effects that undesirably inflate the diffusion tensors ([Arsigny et al., 2007](#)) and impede their interpretation. Consequently, statistical models have adopted a non-Euclidean approach for diffusion tensor analysis. In the analysis reported below we use the Log-Cholesky metric ([Lin, 2019](#)) to analyze diffusion tensors; it is a metric designed to eliminate the swelling effect.

We focus on the hippocampus that plays a central role in Alzheimer’s disease ([Lindberg et al., 2012](#)). In the ADNI study, subjects were invited to visit a center for acquisition of their brain images as well as assessment of their memory, executive functioning and language ability. For each raw diffusion tensor image, a standard preprocessing protocol that includes denoising, eddy current and motion correction, skull stripping, bias correction and normalization is applied. Diffusion tensors for each hippocampal voxel are derived from the preprocessed images. Then the Log-Cholesky mean ([Lin, 2019](#)) of the diffusion tensors is computed. This results in an average diffusion tensor for each raw image. The goal is to study the relation between the average hippocampal diffusion tensor and memory, executive functioning and language ability of the subject. To this end, we utilize the neuropsychological summary scores available from ADNI and documented in [Gibbons et al. \(2012\)](#). In this study we only consider visits that feature both a properly acquired diffusion tensor image and neuropsychological summary scores. After excluding visits with outliers and missing values, there are 590 data tuples of the form (Y, X_1, X_2, X_3) , where Y is the average diffusion tensor, which serves as response, while X_1, X_2, X_3 , standardized to the interval $[0, 1]$, are the predictors and consist of scores for memory, executive functioning and language ability, respectively; 181 are from cognitively normal (CN) subjects and the remainder from patients who were diagnosed as having either early mild cognitive impairment, mild cognitive impairment, late mild cognitive impairment or Alzheimer’s disease (AD). We applied the proposed manifold additive model (1) to the CN and AD groups, respectively.

¹<http://adni.loni.usc.edu/>

The resulting component functions $w_1(x_1), w_2(x_2), w_3(x_3)$ are depicted in Figure 1, where each diffusion tensor is visualized as an ellipsoid whose volume corresponds to the determinant of the tensor, and the color encodes fractional anisotropy which describes the degree of anisotropy of diffusion of water molecules. For a 3×3 symmetric positive-definite matrix A that represents a diffusion tensor, its fractional anisotropy is defined by

$$\text{FA} = \sqrt{\frac{3}{2} \frac{(\rho_1 - \bar{\rho})^2 + (\rho_2 - \bar{\rho})^2 + (\rho_3 - \bar{\rho})^2}{\rho_1^2 + \rho_2^2 + \rho_3^2}}$$

with eigenvalues ρ_1, ρ_2, ρ_3 of A and $\bar{\rho} = (\rho_1 + \rho_2 + \rho_3)/3$. Larger values of fractional anisotropy suggest that movement of the water molecules is constrained by structures such as white matter fibers. In Figure 1 the first component function w_1 suggests that the diffusion tensors are differently associated with memory for the CN and AD groups. In addition, the function w_1 of the CN group overall exhibits larger fractional anisotropy. Similar results are observed for the associations with language ability. In contrast, the association patterns in the two groups are rather similar for executive functioning. The relatively weak association between the average hippocampal diffusion tensor and executive functioning suggests that the hippocampus may play less of a role for executive functioning. In contrast, the significant memory loss and language impairment that accompany Alzheimer's disease appear to be at least partially mediated by the hippocampus. This is in line with previous findings that the integrity of the hippocampus is not only critical to memory (Müller et al., 2005) but also important for the flexible use and processing of language (Duff and Brown-Schmidt, 2012).

Appendix: Proofs

Proof of Proposition 1. First, since \mathcal{M} is a Hadamard manifold, the Riemannian logarithmic map Log_μ and the Lie logarithmic map \mathbf{log} are well defined for all elements of \mathcal{M} . Moreover, for a bi-invariant Lie group, the Riemannian exponential map Exp_e at the identity element e coincides with the Lie exponential map \mathbf{exp} .

For $z \in \mathcal{M}$, let $\mathbf{u} = \mathbf{log}(z) \in \mathfrak{g}$ and denote by U the associated left-invariant vector field. Define $\gamma_\mu(t) = L_\mu(\mathbf{exp}(t\mathbf{u}))$. Then $\gamma'_\mu(t) = U(\mu \oplus \gamma_e(t))$ based on the proof of Lemma 6 in Lin (2019). The fact that $\gamma_e(0) = e$ further leads to $\gamma'_\mu(0) = U(\mu) = \tau_{e,\mu}\mathbf{u}$, where the second equality is due to the fact that the parallel transport of \mathbf{u} is realized by the vector field U . Noting that $\gamma_\mu(0) = \mu$, by the definition of the Riemannian exponential map, $\text{Exp}_\mu \gamma'_\mu(0) = \gamma_\mu(1)$, which leads to $\text{Exp}_\mu \tau_{e,\mu}\mathbf{u} = \ell_\mu(\mathbf{exp}(\mathbf{u})) = \mu \oplus z$. The last equation is equivalent to $\text{Log}_\mu(\mu \oplus z) = \tau_{e,\mu}\mathbf{log}(z)$.

Applying the above with $z = w_1(X_1) \oplus \dots \oplus w_q(X_q) \oplus \zeta$, we have $\text{Log}_\mu Y = \tau_{e,\mu}\mathbf{log}(w_1(X_1) \oplus \dots \oplus w_q(X_q) \oplus \zeta) = \sum_{k=1}^q \tau_{e,\mu}\mathbf{log}w_k(X_k) + \tau_{e,\mu}\mathbf{log}\zeta$, where the second equality stems from $\mathbf{exp}(\mathbf{u} + \mathbf{v}) = \mathbf{exp}(\mathbf{u}) \oplus \mathbf{exp}(\mathbf{v})$ for $\mathbf{u}, \mathbf{v} \in \mathfrak{g}$ and this leads to $\mathbf{log}(u \oplus v) = \mathbf{log}(u) + \mathbf{log}(v)$ for $u, v \in \mathcal{M}$. \square

Proof of Proposition 2. We utilize Corollary 1 of Schötz (2019). We first observe that $d(\hat{\mu}, \mu) = o_P(1)$ according to Theorem 2.3 of Bhattacharya and Patrangenaru (2003) and condition (A1). Then according to

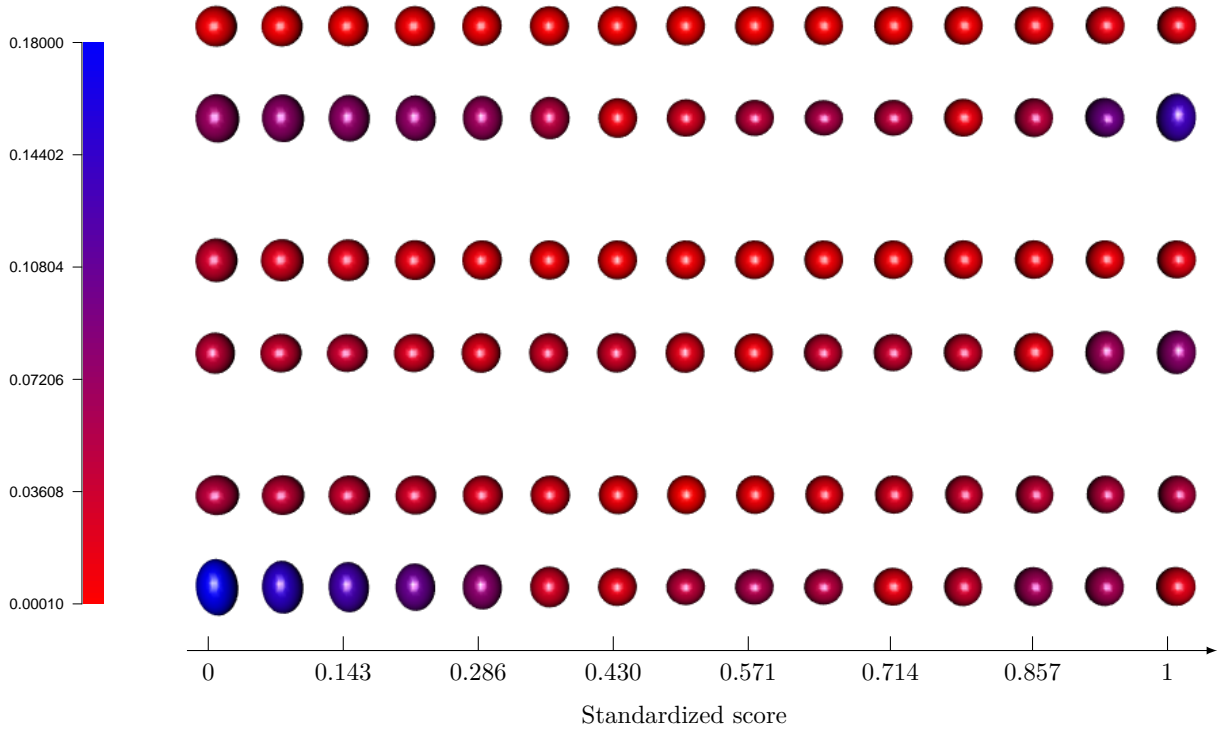


Figure 1: Regression of 3×3 diffusion tensor on memory (X_1), executive functioning (X_2) and language ability (X_3), depicting the estimated additive component functions w_k in model (1): Component function $w_1(X_1)$ for the AD group (Row 1) and the CN group (Row 2); function $w_2(X_2)$ for the AD group (Row 3) and the CN group (Row 4); function $w_3(X_3)$ for the AD group (Row 5) and the CN group (Row 6). The color encodes the level of fractional anisotropy.

Schötz (2019) the growth and entropy conditions are required to hold only in a neighborhood of μ , where the corresponding existence and growth conditions are in assumptions (A1) and (A4), respectively. Condition (A1) implies that F is finite for some point and thus by the triangle inequality for all points in the manifold. If Z is an independent copy of Y , then $\mathbb{E}d^2(Y, Z) \leq 2\mathbb{E}\{d^2(Y, \mu)\} + 2\mathbb{E}\{d^2(\mu, Z)\} = 4F(\mu) < \infty$, and the moment condition of Schötz (2019) follows, as well as the weak quadruple condition, where the latter holds for all Hadamard spaces and bounded spaces. Since a compact manifold is a bounded space, the weak quadruple condition holds for manifolds under (M1) or (M2).

Finally we verify the entropy condition of Schötz (2019). If \mathcal{M} is compact, then its sectional curvature is bounded away from $-\infty$ and $+\infty$. According to the Bishop–Günther inequality (Gray, 2004, Eq. (3.34)), $\text{vol}(B_\epsilon(z)) \geq C_1\epsilon^D$ for all sufficiently small $\epsilon > 0$, where $B_\epsilon(z) = \{y \in \mathcal{M} : d(y, z) < \epsilon\}$ and C_1 is a constant independent of z and ϵ . With this result and equation (3.33) of Gray (2004), the packing number and thus the covering number of $B_\delta(\mu)$ is bounded by $O(\delta^D\epsilon^{-D})$. Therefore, the entropy condition holds for $\alpha = \beta$ for a sufficiently small neighborhood of μ and the result follows. \square

The following lemmas are instrumental to establish Theorems 1 and 2.

Lemma 1. *If Z_1, \dots, Z_n are nonnegative i.i.d. random variables with $\mathbb{E}Z_1^\alpha < \infty$ for some $\alpha > 0$, then $\max_{1 \leq i \leq n} Z_i = O_P(n^{1/\alpha})$.*

Proof of Lemma 1. Let $a_n = n^{1/\alpha}$. By i.i.d. assumption, for $\epsilon > 0$,

$$\begin{aligned} \Pr \left\{ \max_{1 \leq i \leq n} Z_i \leq C a_n \right\} &= (\Pr\{Z_1 \leq C a_n\})^n = (1 - \Pr\{Z_1 > C a_n\})^n \\ &\geq \left(1 - \frac{\mathbb{E}Z_1^\alpha}{C^\alpha a_n^\alpha}\right)^n = \left(1 - \frac{\mathbb{E}Z_1^\alpha}{C^\alpha n}\right)^n \rightarrow e^{-\mathbb{E}Z_1^\alpha / C^\alpha} \\ &\geq 1 - \epsilon \end{aligned}$$

for a sufficiently large C that depends on $\epsilon > 0$. \square

Lemma 2. *Assume the conditions (A1)–(A5) and (B4). If $\mathbb{E}\|\varepsilon\|_\mu^\alpha < \infty$ for some $\alpha > 2$, then*

$$\max_{1 \leq i \leq n} \|\tau_{\hat{\mu}, \mu} \text{Log}_{\hat{\mu}} Y_i - \text{Log}_\mu Y_i\|_\mu = O_P(n^{-(\alpha-2)/(2\alpha)}).$$

Proof of Lemma 2. Using the inequality (5.7) of Kendall and Le (2011), the condition (A5) and $d(\hat{\mu}, \mu) = o_P(1)$ that is guaranteed by Proposition 2, we deduce that, with probability tending to one,

$$\max_{1 \leq i \leq n} \|\tau_{\hat{\mu}, \mu} \text{Log}_{\hat{\mu}} Y_i - \text{Log}_\mu Y_i\|_\mu = O(1) d(\hat{\mu}, \mu) \max_{1 \leq i \leq n} \|\text{Log}_\mu Y_i\|_\mu.$$

By Lemma 1, the moment condition $\mathbb{E}\|\varepsilon\|_\mu^\alpha < \infty$, the compactness of \mathcal{X} and the continuity of f_1, \dots, f_q assumed in (B4), we have $\max_{1 \leq i \leq n} \|\text{Log}_\mu Y_i\|_\mu = O_P(n^{1/\alpha})$. The conclusion of the lemma then follows from Proposition 2. \square

Proof of Theorem 1. We sketch the proof. Define \tilde{m}_j as \hat{m}_j in (5) with $\text{Log}_{\hat{\mu}} Y_i$ being replaced by $\text{Log}_\mu Y_i$. Let $(\tilde{f}_j : 1 \leq j \leq q)$ denote the solution of the system of equations

$$\tilde{f}_k(x_k) = \tilde{m}_k(x_k) - n^{-1} \sum_{i=1}^n \text{Log}_\mu Y_i - \sum_{j:j \neq k} \int_{\mathcal{X}_j} \tilde{f}_j(x_j) \frac{\hat{p}_{kj}(x_k, x_j)}{\hat{p}_k(x_k)} dx_j, \quad 1 \leq k \leq q,$$

subject to the constraints $\int_{\mathcal{X}_k} \tilde{f}_k(x_k) \hat{p}_k(x_k) dx_k = 0$ for $1 \leq k \leq q$. According to the theory of Jeon and Park (2020), under the conditions of the theorem, the solution exists and is unique with probability tending to one. Furthermore, it holds that

$$\begin{aligned} \max_{1 \leq k \leq q} \int_{\mathcal{X}_k} \|\tilde{f}_k(x_k) - f_k(x_k)\|_\mu^2 p_k(x_k) dx_k &= O_P(n^{-4/5}), \\ \max_{1 \leq k \leq q} \int_{\mathcal{X}_k} \|\tilde{f}_k(x_k) - f_k(x_k)\|_\mu^2 p_k(x_k) dx_k &= O_P(n^{-3/5}). \end{aligned} \tag{12}$$

Since the smooth backfitting operation at (4) is linear in response variables and the parallel transport $\tau_{\hat{\mu}, \mu} : T_{\hat{\mu}}(\mathcal{M}) \rightarrow T_\mu(\mathcal{M})$ is also a linear map, we get that $(\tau_{\hat{\mu}, \mu} \hat{f}_j : 1 \leq j \leq q)$ is nothing else than the smooth

backfitting estimator that one gets from the smooth backfitting operation with $\tau_{\hat{\mu},\mu}\text{Log}_{\hat{\mu}}Y_i$ as responses. We claim

$$\max_{1 \leq k \leq q} \int_{\mathcal{X}_k} \|\tau_{\hat{\mu},\mu}\hat{f}_k(x_k) - \tilde{f}_k(x_k)\|_{\mu}^2 p_k(x_k) dx_k = O_P(n^{-(\alpha-2)/\alpha}). \quad (13)$$

The results (12) and (13) give the theorem.

To prove the claim (13), let $\delta_k = \tau_{\hat{\mu},\mu}\hat{f}_k - \tilde{f}_k$. Then, $(\delta_j : 1 \leq j \leq q)$ is the solution of the system of equations

$$\begin{aligned} \delta_k(x_k) = & \tau_{\hat{\mu},\mu}\hat{m}_k(x_k) - \tilde{m}_k(x_k) - n^{-1} \sum_{i=1}^n (\tau_{\hat{\mu},\mu}\text{Log}_{\hat{\mu}}Y_i - \text{Log}_{\mu}Y_i) \\ & - \sum_{j:j \neq k} \int_{\mathcal{X}_j} \delta_j(x_j) \frac{\hat{p}_{kj}(x_k, x_j)}{\hat{p}_k(x_k)} dx_j, \quad 1 \leq k \leq q, \end{aligned}$$

subject to the constraints $\int_{\mathcal{X}_k} \delta_k(x_k) \hat{p}_k(x_k) dx_k = 0$ for $1 \leq k \leq q$. From Lemma 2 it follows that

$$\left\| \tau_{\hat{\mu},\mu}\hat{m}_k(x_k) - \tilde{m}_k(x_k) - n^{-1} \sum_{i=1}^n (\tau_{\hat{\mu},\mu}\text{Log}_{\hat{\mu}}Y_i - \text{Log}_{\mu}Y_i) \right\|_{\mu}^2 = O_P(n^{-(\alpha-2)/\alpha})$$

uniformly for $x_k \in \mathcal{X}_k$ for all $1 \leq k \leq q$. Using the arguments in the proof of Theorem 4.1 in Jeon and Park (2020), we may then prove

$$\sup_{x_k \in \mathcal{X}_k} \|\delta_k(x_k)\|_{\mu}^2 = O_P(n^{-(\alpha-2)/\alpha}). \quad (14)$$

This gives (13). □

Proof of Theorem 2. Let $\tilde{m}_j^A(x_j) = n^{-1}\hat{p}_j(x_j)^{-1} \sum_{i=1}^n K_{h_j}(x_j, X_{ij})\varepsilon_i$. Then we find

$$n^{2/5} (\tilde{f}_j(x_j) - f_j(x_j)) = n^{2/5}\tilde{m}_j^A(x_j) + \tau_{e,\mu} \left(\frac{1}{2}\alpha_j^2 u_2 \cdot \psi_j''(x_j) + \Delta_j(x_j) \right) + o_P(1) \quad (15)$$

for each $x_j \in \text{Int}(\mathcal{X})$ for all $1 \leq j \leq q$, where $u_2 = \int u^2 K(u) du$ and \tilde{f}_j is defined in the proof of Theorem 1. Here, $W_n = o_P(1)$ means $\lim_{n \rightarrow \infty} P(\|W\|_{\mu} > \epsilon) = 0$ for all $\epsilon > 0$. The assertion (15) can be proved along the lines of the proof of Theorem 4.3 in Jeon and Park (2020). The expansion (15) together with (14) entails

$$n^{2/5} \left(\tau_{\hat{\mu},\mu}\hat{f}_j(x_j) - f_j(x_j) \right) = n^{-3/5}\hat{p}_j(x_j)^{-1} \sum_{i=1}^n K_{h_j}(x_j, X_{ij})\varepsilon_i + \theta_j(x_j) + o_P(1), \quad 1 \leq j \leq q.$$

Here, we have used $\alpha > 10$. By identifying $T_{\mu}\mathcal{M}$ and its metric g_{μ} with the Hilbert space \mathbb{H} and the associated inner product $\langle \cdot, \cdot \rangle$ in Jeon and Park (2020), respectively, and utilizing Theorem 1.1 in Kundu et al. (2000), we may prove that the joint distribution of $(n^{-3/5}\hat{p}_j(x_j)^{-1} \sum_{i=1}^n K_{h_j}(x_j, X_{ij})\varepsilon_i : 1 \leq j \leq q)$ converges to $N(\mathbf{x})$. This completes the proof of the theorem. □

Acknowledgments

Data used in preparation of this article were obtained from the Alzheimer’s Disease Neuroimaging Initiative (ADNI) database (adni.loni.usc.edu). As such, the investigators within the ADNI contributed to the design and implementation of ADNI and/or provided data but did not participate in analysis or writing of this report. A complete listing of ADNI investigators can be found at: http://adni.loni.usc.edu/wp-content/uploads/how_to_apply/ADNI_Acknowledgement_List.pdf.

References

- Afsari, B. (2011). Riemannian L^p center of mass: Existence, uniqueness, and convexity. *Proceedings of the American Mathematical Society*, 139(2):655–673.
- Arnaudon, M., Barbaresco, F., and Yang, L. (2013). Riemannian medians and means with applications to radar signal processing. *IEEE Journal of Selected Topics in Signal Processing*, 7(4):595–604.
- Arsigny, V., Fillard, P., Pennec, X., and Ayache, N. (2006). Log-Euclidean metrics for fast and simple calculus on diffusion tensors. *Magnetic Resonance in Medicine*, 56(2):411–421.
- Arsigny, V., Fillard, P., Pennec, X., and Ayache, N. (2007). Geometric means in a novel vector space structure on symmetric positive-definite matrices. *SIAM Journal of Matrix Analysis and Applications*, 29(1):328–347.
- Barmpoutis, A., Vemuri, B. C., Shepherd, T. M., and Forder, J. R. (2007). Tensor splines for interpolation and approximation of DT-MRI with applications to segmentation of isolated rat hippocampi. *IEEE transactions on medical imaging*, 26(11):1537–1546.
- Bhattacharya, R. and Patrangenaru, V. (2003). Large sample theory of intrinsic and extrinsic sample means on manifolds. I. *The Annals of Statistics*, 31(1):1–29.
- Caseiro, R., Henriques, J. F., Martins, P., and Batista, J. (2012). A nonparametric Riemannian framework on tensor field with application to foreground segmentation. *Pattern Recognition*, 45(11):3997–4017.
- Chau, J. and von Sachs, R. (2019). Intrinsic wavelet regression for surfaces of Hermitian positive definite matrices. *arXiv:1808.08764 [stat]*. arXiv: 1808.08764.
- Cornea, E., Zhu, H., Kim, P., and Ibrahim, J. G. (2017). Regression models on Riemannian symmetric spaces. *Journal of the Royal Statistical Society: Series B (Statistical Methodology)*, 79(2):463–482.
- Dai, X. and Müller, H.-G. (2018). Principal component analysis for functional data on Riemannian manifolds and spheres. *The Annals of Statistics*, 46:3334–3361.
- Davis, B. C., Fletcher, P. T., Bullitt, E., and Joshi, S. (2010). Population shape regression from random design data. *International Journal of Computer Vision*, 90(2):255–266.
- Dryden, I. L., Koloydenko, A., and Zhou, D. (2009). Non-Euclidean statistics for covariance matrices, with applications to diffusion tensor imaging. *The Annals of Applied Statistics*, 3(3):1102–1123.

- Duff, M. C. and Brown-Schmidt, S. (2012). The hippocampus and the flexible use and processing of language. *Frontiers in Human Neuroscience*, 6:9.
- Fillard, P., Arsigny, V., Ayache, N., and Pennec, X. (2005). A Riemannian framework for the processing of tensor-valued images. In *International Workshop on Deep Structure, Singularities, and Computer Vision*, pages 112–123.
- Fillard, P., Arsigny, V., Pennec, X., M.Hayashi, K., M.Thompson, P., and Ayache, N. (2007). Measuring brain variability by extrapolating sparse tensor fields measured on sulcal lines. *NeuroImage*, 34(2):639–650.
- Fletcher, P. T. (2013). Geodesic regression and the theory of least squares on Riemannian manifolds. *International Journal of Computer Vision*, 105(2):171–185.
- Fletcher, T. and Joshi, S. (2007). Riemannian geometry for the statistical analysis of diffusion tensor data. *Signal Processing*, 87:250–262.
- Friston, K. J. (2011). Functional and effective connectivity: a review. *Brain Connectivity*, 1(1):13–36.
- Gibbons, L. E., Carle, A. C., Mackin, R. S., Harvey, D., Mukherjee, S., Insel, P., Curtis, S. M., Mungas, D., and Crane, P. K. (2012). A composite score for executive functioning, validated in Alzheimer’s Disease Neuroimaging Initiative (ADNI) participants with baseline mild cognitive impairment. *Brain Imaging and Behavior*, 6(4):517–527.
- Gray, A. (2004). *Tubes*. Springer Basel AG, second edition.
- Han, K., Müller, H.-G., and Park, B. U. (2020). Additive functional regression for densities as responses. *Journal of the American Statistical Association*, 115(530):997–1010.
- Han, K. and Park, B. U. (2018). Smooth backfitting for errors-in-variables additive models. *The Annals of Statistics*, 46(5):216–2250.
- Hein, M. (2009). Robust nonparametric regression with metric-space valued output. In *Advances in Neural Information Processing Systems*, pages 718–726.
- Hinkle, J., Fletcher, P. T., and Joshi, S. (2014). Intrinsic polynomials for regression on Riemannian manifolds. *Journal of Mathematical Imaging and Vision*, 50(1-2):32–52.
- Hua, X., Cheng, Y., Wang, H., Qin, Y., Li, Y., and Zhang, W. (2017). Matrix CFAR detectors based on symmetrized Kullback-Leibler and total Kullback-Leibler divergences. *Digital Signal Processing*, 69(C):106–116.
- Huettel, S. A., Song, A. W., and McCarthy, G. (2008). *Functional Magnetic Resonance Imaging*. Sinauer Associates, 2nd edition.
- Jeon, J. M. and Park, B. U. (2020). Additive regression with Hilbertian responses. *The Annals of Statistics*, page to appear.
- Jung, S., Schwartzman, A., and Groisser, D. (2015). Scaling-rotation distance and interpolation of symmetric positive-definite matrices. *SIAM Journal on Matrix Analysis and Applications*, 36(3):1180–1201.

- Kendall, W. S. and Le, H. (2011). Limit theorems for empirical Fréchet means of independent and non-identically distributed manifold-valued random variables. *Brazilian Journal of Probability and Statistics*, 25(3):323–352.
- Kundu, S., Majumdar, S., and Mukherjee, K. (2000). Central limit theorems revisited. *Statistics and Probability Letters*, 47(3):265–275.
- Lang, S. (1999). *Fundamentals of Differential Geometry*. Springer, New York.
- Le Bihan, D. (1991). Molecular diffusion nuclear magnetic resonance imaging. *Magnetic Resonance Quarterly*, 7(1):1–30.
- Lee, Y. K., Mammen, E., and Park, B. U. (2010). Backfitting and smooth backfitting for additive quantile models. *The Annals of Statistics*, 38(5):2857–2883.
- Lee, Y. K., Mammen, E., and Park, B. U. (2012). Flexible generalized varying coefficient regression models. *The Annals of Statistics*, 40(3):1906–1933.
- Lenglet, C., Rousson, M., Deriche, R., and Faugeras, O. (2006). Statistics on the manifold of multivariate normal distributions: Theory and application to diffusion tensor MRI processing. *Journal of Mathematical Imaging and Vision*, 25(3):423–444.
- Lin, Z. (2019). Riemannian geometry of symmetric positive definite matrices via Cholesky decomposition. *SIAM Journal on Matrix Analysis and Applications*, 40(4):1353–1370.
- Lin, Z. and Müller, H.-G. (2019). Total variation regularized Fréchet regression for metric-space valued data. *arxiv*.
- Lindberg, O., Walterfang, M., Looi, J. C., Malykhin, N., Östberg, P., Zandbelt, B., Styner, M., Velakoulis, D., Örndahl, E., Cavallin, L., and Wahlund, L.-O. (2012). Shape analysis of the hippocampus in alzheimer’s disease and subtypes of frontotemporal lobar degeneration. *Journal of Alzheimer’s Disease*, 30(2):355–365.
- Mammen, E., Linton, O., and Nielsen, J. (1999). The existence and asymptotic properties of a backfitting projection algorithm under weak conditions. *The Annals of Statistics*, 27(5):1443–1490.
- Moakher, M. (2005). A differential geometry approach to the geometric mean of symmetric positive-definite matrices. *SIAM Journal on Matrix Analysis and Applications*, 26(3):735–747.
- Müller, M. J., Greverus, D., Dellani, P. R., Weibrich, C., Wille, P. R., Scheurich, A., Stoeter, P., and Fellgiebel, A. (2005). Functional implications of hippocampal volume and diffusivity in mild cognitive impairment. *Neuroimage*, 28(4):1033–1042.
- Park, B. U., Chen, C.-J., Tao, W., and Müller, H.-G. (2018). Singular additive models for function to function regression. *Statistica Sinica*, 28:2497–2520.
- Pelletier, B. (2006). Non-parametric regression estimation on closed Riemannian manifolds. *Journal of Nonparametric Statistics*, 18(1):57–67.
- Pennec, X. (2006). Intrinsic statistics on Riemannian manifolds: Basic tools for geometric measurements,.

- Journal of Mathematical Imaging and Vision*, 25:127–154.
- Penneç, X. (2020). Manifold-valued image processing with SPD matrices. In *Riemannian Geometric Statistics in Medical Image Analysis*, pages 75–134. Elsevier.
- Penneç, X., Fillard, P., and Ayache, N. (2006). A Riemannian framework for tensor computing. *International Journal of Computer Vision*, 66(1):41–66.
- Petersen, A., Deoni, S., and Müller, H.-G. (2019). Fréchet estimation of time-varying covariance matrices from sparse data, with application to the regional co-evolution of myelination in the developing brain. *The Annals of Applied Statistics*, 13(1):393–419.
- Petersen, A. and Müller, H.-G. (2016). Functional data analysis for density functions by transformation to a Hilbert space. *The Annals of Statistics*, 44(1):183–218.
- Petersen, A. and Müller, H.-G. (2019). Fréchet regression for random objects with Euclidean predictors. *The Annals of Statistics*, 47(2):691–719.
- Pigoli, D., Aston, J. A., Dryden, I. L., and Secchi, P. (2014). Distances and inference for covariance operators. *Biometrika*, 101:409–422.
- Rathi, Y., Tannenbaum, A., and Michailovich, O. (2007). Segmenting images on the tensor manifold. In *Proceedings of Computer Vision and Pattern Recognition*.
- Scheipl, F., Staicu, A.-M., and Greven, S. (2015). Functional additive mixed models. *Journal of Computational and Graphical Statistics*, 24(2):477–501.
- Schötz, C. (2019). Convergence rates for the generalized Fréchet mean via the quadruple inequality. *Electronic Journal of Statistics*, 13:4280–4345.
- Shi, X., Styner, M., Lieberman, J., Ibrahim, J. G., Lin, W., and Zhu, H. (2009). Intrinsic regression models for manifold-valued data. In *Medical Image Computing and Computer-Assisted Intervention - MICCAI*, volume 12, pages 192–199.
- Steinke, F., Hein, M., and Schölkopf, B. (2010). Nonparametric regression between general Riemannian manifolds. *SIAM Journal on Imaging Sciences*, 3(3):527–563.
- Stone, C. J. (1985). Additive regression and other nonparametric models. *The Annals of Statistics*, 13:689–705.
- Sturm, K.-T. (2003). Probability measures on metric spaces of nonpositive curvature. In *Heat kernels and analysis on manifolds, graphs, and metric spaces (Paris, 2002)*, vol. 338 of *Contemporary Mathematics*, pages 357–390. American Mathematical Society, Providence, RI.
- Yu, K., Park, B. U., and Mammen, E. (2008). Smooth backfitting in generalized additive models. *The Annals of Statistics*, 36(1):228–260.
- Yuan, Y., Zhu, H., Lin, W., and Marron, J. S. (2012). Local polynomial regression for symmetric positive definite matrices. *Journal of Royal Statistical Society: Series B (Statistical Methodology)*, 74(4):697–719.

- Zhou, D., Dryden, I. L., Koloydenko, A. A., Audenaert, K. M., and Bai, L. (2016). Regularisation, interpolation and visualisation of diffusion tensor images using non-Euclidean statistics. *Journal of Applied Statistics*, 43(5):943–978.
- Zhu, H., Chen, Y., Ibrahim, J. G., Li, Y., Hall, C., and Lin, W. (2009). Intrinsic regression models for positive-definite matrices with applications to diffusion tensor imaging. *Journal of the American Statistical Association*, 104(487):1203–1212.